hamlet, a Binary Genetic Switch Between Single- and Multiple-Dendrite Neuron Morphology

Adrian W. Moore, Lily Yeh Jan, Yuh Nung Jan*

The dendritic morphology of neurons determines the number and type of inputs they receive. In the *Drosophila* peripheral nervous system (PNS), the external sensory (ES) neurons have a single nonbranched dendrite, whereas the lineally related multidendritic (MD) neurons have extensively branched dendritic arbors. We report that *hamlet* is a binary genetic switch between these contrasting morphological types. In *hamlet* mutants, ES neurons are converted to an MD fate, whereas ectopic *hamlet* expression in MD precursors results in transformation of MD neurons into ES neurons. Moreover, *hamlet* expression induced in MD neurons undergoing dendrite outgrowth drastically reduces arbor branching.

In *Drosophila* embryos, a single external sensory organ precursor (ESOP) cell gives rise to an ES neuron and an MD neuron through a stereotypical series of asymmetric cell divisions. The IIA daughter of the ESOP divides once to produce a trichogen and a tormagen, the two external support cells of the ES neuron. The IIB daughter of the ESOP generates an MD neuron and the IIIB cell, which divides to form an ES neuron and a glia (*1*) (Fig. 1A).

In a genetic screen designed to identify mutants in *Drosophila* embryonic dendrite development (*2*), we isolated a larval lethal mutant that appeared to affect determination of cells descended from the IIB precursor of the ESOP lineage. We named this mutation *hamlet* (*ham*) after the "To be or not to be" soliloquy in the Shakespeare play of the same name.

In embryos homozygous for the *ham*^{1} mutation, supernumerary MD neurons were evident in each PNS cluster of the embryo, as well as a concomitant decrease in the number of ES neurons. For example, in the wild-type dorsal PNS cluster there are 13 neurons: five ES neurons, which express the pan-neural marker ELAV (embryonic lethal abnormal visual system), and eight MD neurons, which express ELAV and the enhancer-trap E7-2-36, a pan-MD marker (*3*). In *ham*^{1} mutants, however, the number of MD neurons was increased up to 13 and the number of ES neurons decreased (Fig. 1, B to E).

Do these extra MD neurons arise at the expense of their sibling ES neurons? To answer this question, we concentrated on the ventral pore sensory organs (vp1 to vp4a) because their lineage is fully described and each organ develops clearly spaced from those surrounding it (*1*). We labeled these organs with an antibody to CUT, which is expressed in all cells of the lineage. In the five differentiated cells of the lineage, CUT is expressed at low levels in the ES and MD neurons and at a much higher level in the trichogen, tormagen, and glia (*4*). In addition, we labeled with antibodies to the MD marker

Howard Hughes Medical Institute, Departments of Physiology and Biochemistry, University of California, San Francisco, CA 94143, USA.

*To whom correspondence should be addressed. E-mail: ynjan@itsa.ucsf.edu

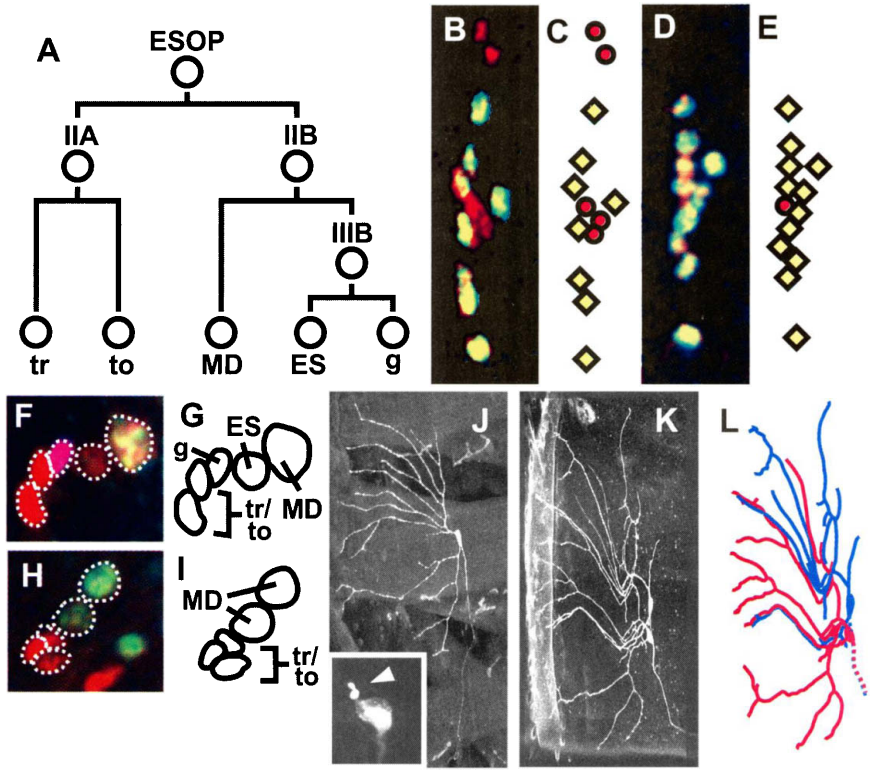

Fig. 1. Transformation of ES neurons to MD neurons in the *ham*^{1} ESOP lineage. In this and other figures, dorsal is up and anterior is to the left. (**A**) Diagram of the ESOP lineage. Abbreviations: ES, external sensory neuron; MD, multidendritic neuron; tr, trichogen; to, tormagen; g, glia. (**B** to **E**) A wild-type (B) and *ham*^{1} homozygous (D) embryonic abdominal dorsal cluster, early stage 17. Cells were labeled with fluorescent antibodies to ELAV (red), which labels all sensory neurons, and to E7-2-36 (green), which labels all MD neurons. The wild-type cluster in (B) contains eight MD neurons and five ES neurons; the *ham*^{1} homozygous embryo in (D) contains 12 MD neurons and one ES neuron. (C) and (E) are representations of (B) and (D), respectively (ES neurons, red circles; MD neurons, yellow diamonds). (**F** to **I**) vp4a organs at embryonic stage 13 (cells were labeled with fluorescent antibodies to CUT, red; PROS, blue; E7-2-36, green). A wild-type organ (F and G) consists of five cells; two external cells (trichogen and tormagen) have high levels of CUT expression, one glial cell expresses high levels of CUT and PROS, one ES neuron has weak CUT expression, and one MD neuron expresses E7-2-36 and weak CUT. In a *ham*^{1} homozygous embryo (H and I) there are also five cells. The ESOP lineage produces three external cells with high levels of CUT but no PROS staining and two MD neurons with E7-2-36 and weak CUT expression. (**J** to **L**) Dendritic arborizations of an MD neuron (in this case ddaD) in the third-instar larval dorsal cluster, visualized using mCD8-gfp via the MARCM system. A wild-type clone is shown in (J); in the inset, a magnified image of a dorsal ES neuron at this stage, the single short dendrite is marked with an arrowhead. In a homozygous *ham*^{1} clone (K), two MD neurons are produced from the ESOP lineage and both neurons have extensive arbors; (L) is an illustration tracing the dendrites of the neurons in (K), one in blue and the other in red.

E7-2-36 and PROSPERO (PROS) (*5*), which is expressed in the IIB cell and its descendants and remains expressed in the differentiated glia. In *ham*^{1} mutants the vp ESOP lineage division pattern appeared normal and produced five cells; however, in the differentiated organ of these mutants, the ES neuron and glia were lost. A second MD neuron appeared in the position normally occupied by the ES neuron, and a third external cell (trichogen) in the position normally occupied by the glia (Fig. 1, F to I). Taken together, these observations indicate that the daughter cells of the IIIB cell are transformed to an MD neuron and a trichogen in *ham*^{1} mutants.

To test whether the supernumerary MD neurons can extend the characteristic complex branched dendritic arbor, we generated *ham*^{1}/*ham*^{1} MARCM (mosaic analysis with a repressible cell marker) clones in the ESOP lineage (*6, 7*). In this analysis, clones of positively marked neurons are derived from a single mitotic recombination event within the ESOP lineage. In wild-type clones of all PNS clusters, MD neurons either label alone, representing a clone derived from recombination within the IIB cell, or in association with an ES neuron, representing recombination at the level of the ESOP cell or its precursors (Fig. 1J). In *ham*^{1} homozygous clones of all PNS clusters, either one or two MD neurons are labeled. In the latter case, one of these neurons must represent the transformed ES cell. Both of these neurons have the arbors characteristic of MD neurons specific to the location at which they arise (Fig. 1, K and L). Thus, in *ham*^{1} the MD neuron transformed from an ES neuron has a full MD arbor morphology. Additionally, this analysis also shows that *ham* functions in a cell-autonomous manner within the ESOP lineage.

To determine the identity of the *ham* gene that allows the ES neuron and glia to adopt their normal cell fate, we used genetic complementation to map the *ham*^{1} mutation between the *tup* and *msl1* genes on the second chromosome (Fig. 2A). Because the Gadfly database (*8, 9*) predicts 27 putative transcripts between *tup* and *msl1*, we used a polymerase chain reaction to amplify digoxigenin-labeled DNA probes representing each one of these transcripts from embryonic cDNA; we then used these probes for mRNA in situ hybridization of a stage 0 to stage 16 embryo collection. Of these 27 putative transcripts, only CG10568 is expressed in the developing PNS of the embryo. We expected that *ham* expression might be largely PNS specific because *ham*^{1} mutants have no defects in muscle, gut, trachea, central nervous system, or cuticle formation, and because *ham* functions in a cell-autonomous manner within the PNS ESOP lineage. We therefore pursued CG10568 as the candidate likely to be disrupted in these mutants.

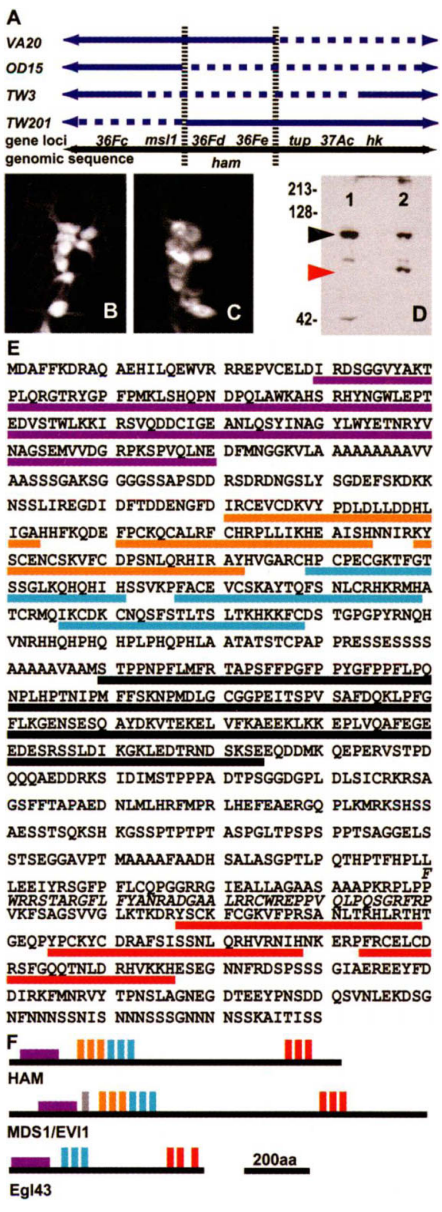

Fig. 2. Mapping and sequence analysis of *ham*. (**A**) A diagram illustrating where the *ham*^{1} mutation maps in relation to several deficiencies and genetic markers. The genomic DNA missing from each deficiency is indicated by a blue dotted line. (**B** and **C**) dsRNAi analysis with the putative transcript CG10568. In a wild-type abdominal dorsal cluster (B), one tracheal neuron and seven MD neurons express green fluorescent protein (GFP). In embryos injected with dsRNA corresponding to 600 bp of CG10568 (C), as many as 11 GFP-positive neurons were seen. For the dsRNA-injected group, $n = 23$, mean = 9.0, SD = 1.2; for the buffer-injected group, $n = 23$, mean = 7.6, SD = 0.9; $P < 10^{-3}$. (**D**) Western blot probed with an antibody to HAM; molecular mass markers in kD are shown. In a wild-type embryo extract (lane 1), a single major band of the predicted size for HAM (109 kD) was detected (black arrowhead); extracts from *ham*^{1} heterozygous embryos (lane 2) contained this band as well as a band of the size predicted for the truncated protein produced in *ham*^{1} (red arrowhead). A faint band corresponding to either a nonspecific interaction or a HAM degradation product is also present in both lanes. (**E** and **F**) The amino acid sequence of HAM (E) (the predicted alterations in amino acid sequence and truncation of this protein in the ham^1 mutant are shown in italics below the sequence) and an illustration of the homology of HAM, MDS1/EVI1, and Egl43 (F). Color code for domains of interest: purple, PR domain; orange/blue/red, zinc fingers (ZF); black, the region to which the antibody to HAM was generated. Color coding of HAM, MDS1/EVI1, and Egl43 indicates conservation of specific domains of identity. The degrees of identity and similarity are as follows: orange + blue, HAM (ZF1–6) vs. MDS1/EVI1 (ZF2–7), 61% identical, 73% similar; blue, HAM (ZF3–6) vs. MDS1/EVI1 (ZF4–7), 78% identical, 84% similar; red, HAM (ZF7–9) vs. MDS1/EVI1 (ZF8–10), 86% identical, 96% similar; blue, HAM (ZF4–6) vs. Egl43 (ZF1–3), 50% identical, 67% similar; blue, HAM (ZF4–5) vs. Egl43 (ZF1–2), 65% identical, 81% similar; red, HAM (ZF7–9) vs. Egl43 (ZF4–6, gap between ZF5 and ZF6 removed), 81% identical, 89% similar; purple, HAM (PR) vs. MDS1/EVI1 (PR), 23% identical, 41% similar. Single-letter abbreviations for amino acid residues: A, Ala; C, Cys; D, Asp; E, Glu; F, Phe; G, Gly; H, His; I, Ile; K, Lys; L, Leu; M, Met; N, Asn; P, Pro; Q, Gln; R, Arg; S, Ser; T, Thr; V, Val; W, Trp; and Y, Tyr.

Two lines of investigation revealed that CG10568 corresponds to the *ham* transcript. First, we used probes derived from CG10568 to isolate from an embryonic library (LD) (*10*) a full-length cDNA corresponding to eight exons spanning about 25 kb of genomic DNA. The predicted protein is 990 amino acids with a mass of 109 kD. It contains an NH_2-terminal PRD1-BF1-RIZ1 homology (PR) domain (*11, 12*) followed by a group of six zinc fingers (ZF) and a group of three additional ZFs at the COOH-terminus (Fig. 2, E and F). Sequencing of the genomic region encoding this transcript in *ham*^{1} mutants revealed a single base pair loss at G^{2866}, which leads to an altered amino acid composition for 41 residues after the mutation site and a truncation that removes the three COOH-terminal ZFs. This mutation thus gives rise to a protein predicted to be 88 kD (represented in italics below the wild-type sequence in Fig. 2E). We raised polyclonal antibodies in guinea pigs against a unique 135–amino acid portion of the predicted HAM protein (Fig. 2E). On a Western blot, the antibody detected a protein of about 110 kD in wild-type embryos. In *ham*^{1} heterozygotes the same band was visible in addition to a protein band at about 90 kD, most likely corresponding to the truncated protein produced by the *ham*^{1} allele (Fig. 2D).

Second, double-stranded RNA interference (dsRNAi) could phenocopy the *ham*^{1} mutation (*13*). dsRNA corresponding to the same sequence used in the CG10568 mRNA in situ was injected into the posterior pole of

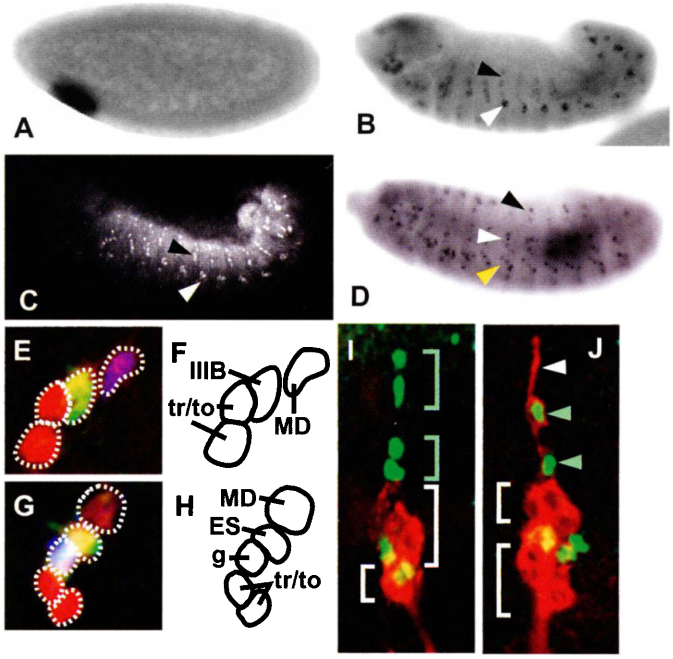

Fig. 3. *ham* expression during embryogenesis. (**A**, **B**, and **D**) *ham* mRNA in situ and (**C**) staining with antibody to HAM shows a similar expression pattern in the developing embryo. In a stage 5 embryo (A), *ham* is expressed in a ventral patch in the cephalic region. In stage 12 embryos (B and C), *ham* RNA and protein exhibit the same expression pattern; they are expressed strongly in the lateral (white arrowhead) and weakly in the dorsal (black arrowhead) PNS clusters. In a stage 13 embryo (D), *ham* expression in the lateral cluster (white arrowhead) is reduced, showing the transient nature of this expression, while in the dorsal (black arrowhead) and ventral (yellow arrowhead) clusters, gene expression levels have become stronger. (**E** to **H**) Expression of HAM in the developing vp4a cell cluster (fluorescently labled with antibodies to CUT, red; PROS, blue; HAM, green). In (E) and (F), the IIIB cell expresses HAM and a low level of CUT while the MD neuron expresses PROS (transiently) and a low level of CUT. In (G) and (H), the daughters of the IIIB cell both express HAM. The ES neuron expresses HAM and a low level of CUT; the glia expresses HAM, PROS, and a high level of CUT. By this stage, the MD neuron no longer expresses PROS. (**I** and **J**) Dynamic HAM expression in the developing dorsal cluster of stage 14–15 embryos (Cells were labeled with fluorescent antibodies to HAM, green, and 22C10, red). 22C10 labels all sensory neurons and is switched on during the process of neuron differentiation. (I) At this stage, 22C10 expression is seen in the MD neurons (white bracket) but not the ES neurons. The ES neuron and glia (one of each contained within each green bracket) both express HAM. (J) As cell differentiation proceeds, HAM is lost from the glia, and the ES neuron (green arrowhead) continues to express HAM and also begins to express 22C10, which labels the extending dendrite (white arrowhead).

embryos carrying the MD marker 109(2)80-*gal4* driving UAS-*gfp* (*2*) or the MD marker E7-2-36 (*3*). In embryos containing 109(2)80-*gal4* driving UAS-*gfp*, CG10568 dsRNAi led to a consistent and significant ($P < 10^{-3}$) increase in the number of MD neurons in the dorsal cluster of these embryos (up to 11 neurons) (Fig. 2C) compared with uninjected embryos (8 neurons) (Fig. 2B) and the buffer-injected control embryos (7 or 8 neurons). This increase was at the expense of ES neurons, as revealed by CG10568 dsRNAi in embryos labeled with antibodies to the MD marker E7-2-36 and the pan-neural marker ELAV (fig. S1).

These findings verify that CG10568 corresponds to the *ham* gene. The *ham*^{1} allele is either a genetic null or strong hypomorph, as embryos containing one copy of the *ham*^{1} mutation and one copy of a deficiency (*Df(2L)OD15*) deleting the gene have the same highly penetrant phenotype as *ham*^{1} homozygotes. Moreover, dsRNAi with *ham* RNA abolishes all HAM protein expression in the injected embryo and phenocopies the *ham*^{1} allele (Fig. 2, B and C) (fig. S1 and table S1).

ham is expressed in a ventral patch in the cephalic region of the embryo from stage 5 (Fig. 3A) and continues to be expressed in the cephalic region through stage 15. It is expressed in the developing PNS from stage 11 through 15 and shows transient expression in each PNS cluster (Fig. 3, B and D). The HAM protein has the same expression profile as the mRNA and has a nuclear localization (Fig. 3C). In the ESOP lineage, it is first expressed in the IIIB cell (Fig. 3, E and F) and is inherited by both the ES neuron and glia daughter cells after IIIB division (Fig. 3, G to I; Fig. 4A). Although

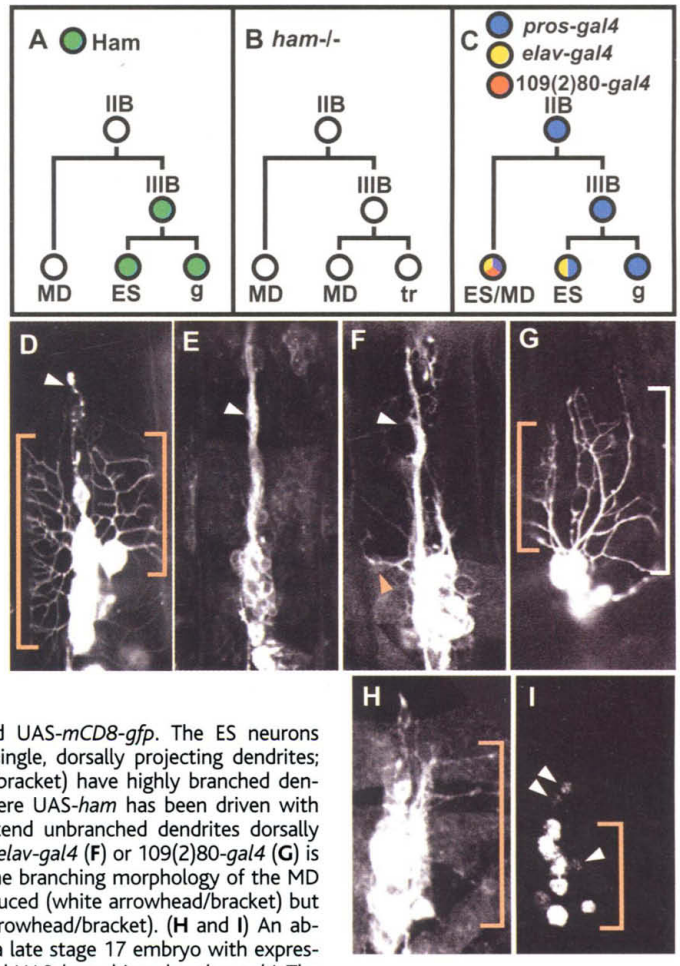

Fig. 4. Ectopic expression of HAM in the MD neurons causes an MD- to ES-like morphology transition. (**A**) An illustration of HAM expression (green) in a wild-type ESOP lineage. (**B**) In a *ham*^{1} homozygous embryo, the IIB cell lineage gives rise to two MD neurons and one trichogen cell. (**C**) When HAM is expressed in the IIB cell [via *pros-gal4* (blue)], the MD neurons are converted to ES neurons. Postmitotic HAM expression in an MD neuron, via either *elav-gal4* (yellow) or 109(2)80-*gal4* (orange), suppresses the dendritic branching of the MD neuron. (**D**) An abdominal dorsal cluster of a stage 17 embryo with the neurons/dendrites visualized by *elav-gal4* and UAS-*mCD8-gfp*. The ES neurons (white arrowhead) have single, dorsally projecting dendrites; the MD neurons (orange bracket) have highly branched dendrites. (**E**) In embryos where UAS-*ham* has been driven with *pros-gal4*, all neurons extend unbranched dendrites dorsally (white arrowhead). When *elav-gal4* (**F**) or 109(2)80-*gal4* (**G**) is used to drive UAS-*ham*, the branching morphology of the MD arbors is substantively reduced (white arrowhead/bracket) but not eliminated (orange arrowhead/bracket). (**H** and **I**) An abdominal dorsal cluster of a late stage 17 embryo with expression of UAS-*mCD8-gfp* and UAS-*ham* driven by *elav-gal4*. The neurons and dendrites are stained with fluorescent antibodies to detect E7-2-36 and mCD8 expression. The dendrites have reduced branching and project dorsally (H) (orange bracket) as compared to the wild type (D). However, the MD neurons still express E7-2-36 at high levels (I) (orange bracket). At this late embryonic stage, as in a wild-type control, the ES neurons have begun to express this marker but at much lower levels (white arrowheads).

HAM quickly disappears in the differentiating glia, it continues to be expressed by the ES neuron during initial dendrite extension (Fig. 3J), indicating that it may be active both pre- and postmitotically in these neurons. HAM levels become undetectable as further dendrite elaboration occurs. This expression pattern is consistent with the notion that HAM is required for proper cell fate specification of the IIIB lineage (Fig. 4, A and B), and (notably, given the nature of our screen) is required for the dendritic morphogenesis of the ES neuron.

To determine whether ectopic HAM expression can alter cell fate, we cloned the full-length *ham* cDNA into the pUAST vector and created UAS-*ham* transgenic flies (*14*). Ectopic HAM expression in the IIB precursor of the MD neuron using *pros-gal4* (Fig. 4C) resulted in loss of labeling for the E7-2-36 MD marker in all embryonic PNS neurons, indicating an MD-to-ES marker transformation. To test whether the dendrite morphology of these neurons also reflects an MD-to-ES transformation, we used *elav-gal4* (Fig. 4C) driving UAS-*gfp* to visualize dendrites. In the wild-type dorsal cluster of stage 17 embryos, there are several neurons with multiply branched dendrites (i.e., MDs) and two dorsal ES neurons, each with a single dorsally projecting dendrite (Fig. 4D). In embryos where both *pros-gal4* and *elav-gal4* drive UAS-*ham* and UAS-*mCD8-gfp* in parallel, the multiple dendritic arbor of the MD neurons has clearly been transformed (Fig. 4E); the dendrites of all neurons in the cluster are unbranched and project dorsally.

Given that HAM is expressed in the postmitotic ES neuron during dendrite extension, we investigated whether postmitotic expression of HAM in an MD neuron can alter its dendrite morphology. We used *elav-gal4* to drive UAS-*ham* and UAS-*mCD8-gfp* in parallel in the embryo (Fig. 4C). Indeed, we found that postmitotic expression of HAM in the MD neurons drastically reduced dendritic branching, leading to arbors with a structure intermediate between that of MD and ES neurons (Fig. 4F). In addition, these neurons still expressed the MD marker E7-2-36 at high levels, indicating that these neurons have transformed dendrite morphology but not cell fate (Fig. 4, H and I). To investigate this effect further, we used the MD-specific driver 109(2)80-*gal4* (Fig. 4C) to drive UAS-*gfp* and UAS-*ham*. In these embryos 109(2)80-*gal4* remains active, implying that the neurons in which it is expressed remain MD; however, the branching of dendrites in these MD neurons is clearly reduced (Fig. 4G). These two lines of evidence illustrate that postmitotic expression of HAM in MD neurons does not switch the fate of these neurons to ES but does still act to suppress the formation of complex dendritic arbors.

The PR domain and bipartite multiple ZF structure define a small family of proteins, of which HAM is the sole member described in *Drosophila* (*15*). The sequence of the PR domain and ZFs as well as the overall domain structure are conserved between HAM and two other proteins, human MDS1/EVI1 (myelodysplasia syndrome 1/ectopic viral integration 1) (*16*) and *Caenorhabditis elegans* Egl43 (egg laying defective 43) (*17*) (Fig. 2, E and F). Both are implicated in neural development. MDS1/EVI1 was originally isolated because ectopic expression of EVI1 alone, leading to a protein still containing the ZFs but lacking the PR domain, can cause leukemia (*16, 18*). A partial disruption of the *Mds1/Evi1* locus in mouse, however, leads to mid-gestation lethality. Among multiple defects in these embryos are regions of hypocellularity in the neuroectoderm and a failure of peripheral nerve formation (*19*). Egl43 is required for hermaphrodite-specific neuron migration and phagemid sensory neuron development. The defect in phagemid neuron development is intriguing because these neurons fail to fill with dye through normally exposed sensilla, a phenotype that could be attributable to a failure of correct dendrite formation (*17, 20*). Thus, it will be interesting to investigate whether *MDS1/EVI1* or *Egl43*, like *ham*, have a role in dendrite specification.

To our knowledge, *ham* represents the only binary genetic switch identified that acts to repress a multiple dendritic arbor and promote single-dendrite morphology. We expect that HAM is a transcription factor; it has a nuclear subcellular distribution, and MDS1/EVI1 can bind DNA and regulate transcription (*21*). HAM must exert its effect in a short developmental window, as its expression is initiated in the IIIB neural precursor and continues only during the initial stages of ES neuron differentiation. Given this short period of activity, it is likely that HAM induces a cascade of events. Its transcriptional targets are likely to include key players in the genetic determination of dendrite morphology that act to repress dendritic branching and promote single- over multiple-dendrite morphology.

References and Notes

1. V. Orgogozo, F. Schweisguth, Y. Bellaiche, *Development* **128**, 631 (2001).
2. F. B. Gao, J. E. Brenman, L. Y. Jan, Y. N. Jan, *Genes Dev.* **13**, 2549 (1999).
3. E. Bier *et al.*, *Genes Dev.* **3**, 1273 (1989).
4. K. Blochlinger, R. Bodmer, L. Y. Jan, Y. N. Jan, *Genes Dev.* **4**, 1322 (1990).
5. H. Vaessin *et al.*, *Cell* **67**, 941 (1991).
6. T. Lee, L. Luo, *Neuron* **22**, 451 (1999).
7. See supporting data on *Science* Online.
8. M. D. Adams *et al.*, *Science* **287**, 2185 (2000).
9. Berkeley *Drosophila* Genome Project (www.fruitfly.org/annot).
10. LD library provided by Berkeley *Drosophila* Genome Project (www.fruitfly.org/EST), probed by standard protocols.
11. S. Huang, *Cell* **78**, 9 (1994).
12. S. Huang, G. Shao, L. Liu, *J. Biol. Chem.* **273**, 15933 (1998).
13. L. Misquitta, B. M. Paterson, in Drosophila *Protocols*, W. Sullivan, M. Ashburner, R. S. Hawley, Eds. (Cold Spring Harbor Laboratory Press, Cold Spring Harbor, NY, 2000), pp. 361–372.
14. P. van Roessel, A. H. Brand, in Drosophila *Protocols*, W. Sullivan, M. Ashburner, R. S. Hawley, Eds. (Cold Spring Harbor Laboratory Press, Cold Spring Harbor, NY, 2000), pp. 439–447.
15. G. L. Jiang, S. Huang, *Histol. Histopathol.* **15**, 109 (2000).
16. S. Fears *et al.*, *Proc. Natl. Acad. Sci. U.S.A.* **93**, 1642 (1996).
17. G. Garriga, C. Guenther, H. R. Horvitz, *Genes Dev.* **7**, 2097 (1993).
18. K. Morishita *et al.*, *Cell* **54**, 831 (1988).
19. P. R. Hoyt *et al.*, *Mech. Dev.* **65**, 55 (1997).
20. C. Desai, G. Garriga, S. L. McIntire, H. R. Horvitz, *Nature* **336**, 638 (1988).
21. J. Soderholm, H. Kobayashi, C. Mathieu, J. D. Rowley, G. Nucifora, *Leukemia* **11**, 352 (1997).

22. We thank F.-B. Gao, J. Brenman, and W. Grueber for reagents and advice; S. Albin, S. Goulding, and N. Justice for critical reading of the manuscript; and the Bloomington Stock center, J. Roote, and C. Nüsslein-Volhard for *Drosophila* stocks. Supported by a Wellcome Trust International Prize Traveling Research Fellowship (A.W.M.) and by NIH grant R01NS40929. Y.N.J. and L.Y.J. are Howard Hughes investigators.

Supporting Online Material

www.sciencemag.org/cgi/content/full/297/5585/1355/DC1

Materials and Methods

Fig. S1

Table S1

29 March 2002; accepted 9 July 2002